

## Real Time Dual-Channel Multiplex SERS Ultradetection

Sara Abalde-Cela,<sup>†,‡</sup> Chris Abell,<sup>†</sup> Ramón A. Alvarez-Puebla,<sup>\*,||,§</sup> and Luis M. Liz-Marzán<sup>\*,‡,⊥,♯</sup>

<sup>†</sup>Department of Chemistry, University of Cambridge, Lensfield Road, Cambridge CB2 1EW, United Kingdom

<sup>‡</sup>Department of Physical Chemistry, Universidade de Vigo, Vigo, Spain

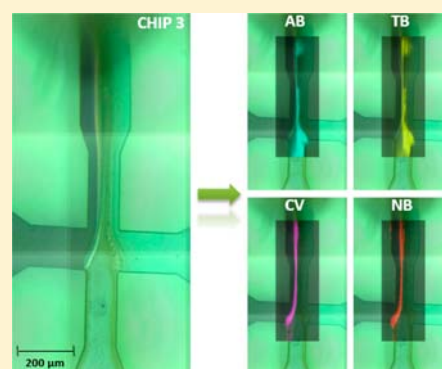
<sup>||</sup>Departamento de Química Física e Inorgánica, Universitat Rovira i Virgili and Centro de Tecnologia Química de Catalunya, Carrer de Marcel·lí Domingo s/n, 43007 Tarragona, Spain

<sup>§</sup>ICREA, Passeig Lluís Companys 23, 08010 Barcelona, Spain

<sup>⊥</sup>Bionanoplasmonics Laboratory, CIC biomaGUNE, Paseo de Miramón 182, 20009 Donostia - San Sebastián, Spain

<sup>♯</sup>Ikerbasque, Basque Foundation for Science, 48011 Bilbao, Spain

**ABSTRACT:** Surface-enhanced Raman scattering (SERS) can be combined with microfluidics for rapid multiplex analyte screening. Through combination of the high intensity and complex signals provided by SERS with the flow characteristics of microfluidic channels, we engineered a microdevice that is capable of monitoring various analytes from different sources in real time. Detection limits down to the nM range may allow the generation of a new family of devices for remote, real time monitoring of environmental samples such as natural or waste waters and application to the high-throughput screening of multiple samples in healthcare diagnostics.



**SECTION:** Plasmonics, Optical Materials, and Hard Matter

Microfluidic devices have found wide application in the integration of ultrasensitive chemical and biological analysis systems.<sup>1,2</sup> On-chip detection offers the advantage of providing real time information about chemical reactions and species present in a fluid sample, even though extremely small volumes are used.<sup>3,4</sup> In the early development stages of microfluidic detection, off-chip methods, such as high-performance liquid chromatography (HPLC) or mass spectrometry (MS),<sup>5,6</sup> were widely used to identify the minute amounts of chemical species present in the small volume of a microfluidic chip. The static nature of these measurements was overcome by moving into on-chip detection.<sup>7</sup> Techniques such as fluorescence,<sup>8</sup> UV–visible spectroscopy,<sup>9</sup> chemiluminescence,<sup>10</sup> electroluminescence,<sup>11</sup> or thermal lens microscopy<sup>12</sup> have been widely implemented into microfluidic platforms to produce analytical devices during the past 2 decades.<sup>13</sup> Fluorescence detection has been the most widely used and representative technique due to its high sensitivity, low cost, and ease of use.<sup>14,15</sup> Nevertheless, this technique presents some limitations, including the broadness of the fluorescence peaks, which can overlap with each other when multiplex detection is desired. These challenges have pushed researchers to implement alternative on-chip ultradetection techniques.<sup>15–17</sup>

Generally speaking, the ideal analytical tool should allow users to investigate a sample for a number of targets simultaneously in a single run/cycle of the assay within the same sample, so that a rapid and accurate description of the

sample is obtained. In this context, surface-enhanced Raman scattering (SERS) spectroscopy has gained increasing relevance as a potential multiplex detection technique.<sup>18</sup> In SERS, the specific Raman scattering signals of the target molecules are largely enhanced due to the coupling of their vibrational modes to the localized surface plasmon resonances (LSPRs) excited in nearby plasmonic nanoparticles. This signal enhancement brings about multiple benefits, such as ultrasensitive detection (down to the zeptomolar regime) or a significant decrease of the required acquisition times for less dilute samples, thereby facilitating real time applications such as high-throughput screening. SERS detection is usually carried out in a static configuration, where the analytes are retained either at the surface of solid thin films or on colloidal particles in solution, and most often a single analyte can be identified in one run. However, combining the high intensity of the signals obtained with this technique and the modern developments in the fields of microfluidics and optical spectroscopy (e.g., 2D CCD cameras) enables the real time (online) monitoring of continuous flows.<sup>19</sup> In fact, online SERS detection<sup>20</sup> has been demonstrated using Y- or T-shaped microfluidic devices for a number of interesting analytes including pesticides<sup>21</sup> and metal ions<sup>22,23</sup> in water or explosives<sup>24</sup> and pollutants<sup>25</sup> from air

**Received:** November 9, 2013

**Accepted:** November 27, 2013

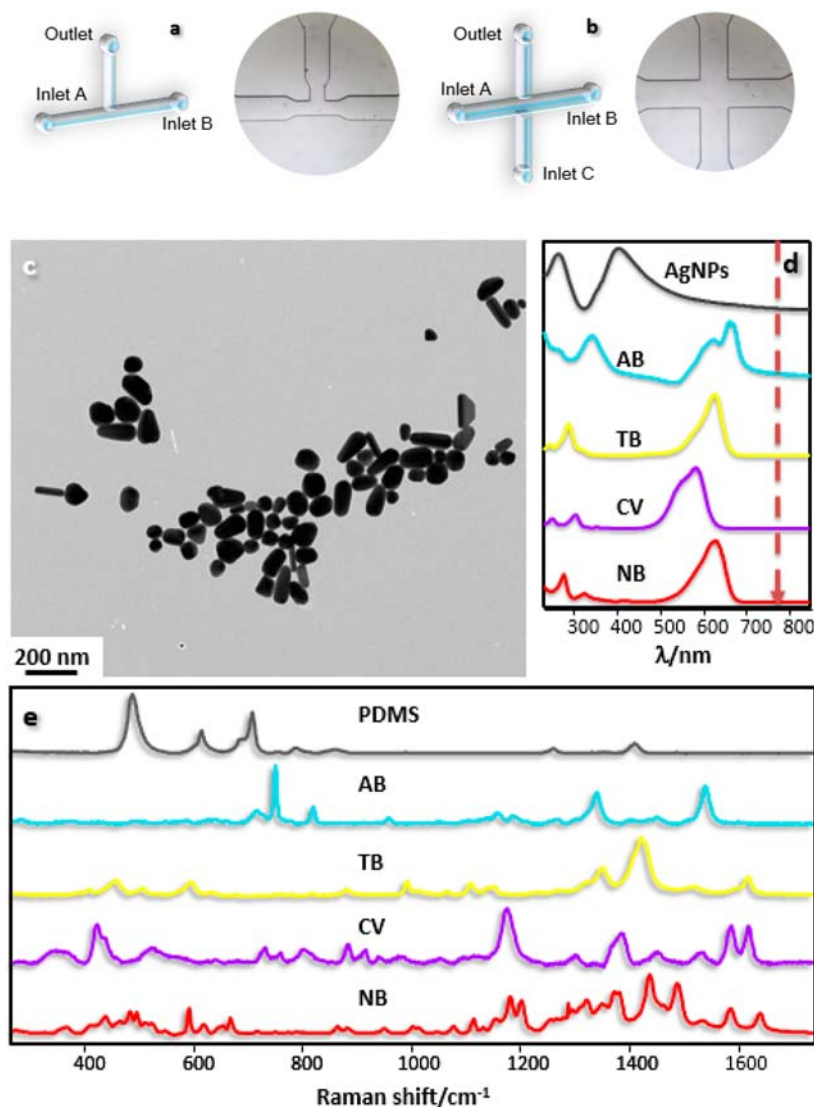


**Figure 1.** (a,b) Scheme and photographs of the microfluidic devices designed for the different experiments, with dimensions of  $150 \times 75$  and  $300 \times 150 \mu\text{m}^2$  in width  $\times$  height for the T- and +-shaped chips, respectively. (c) TEM micrograph of the silver nanoparticles used as the optically active substrate. (d) UV-vis spectra of the NPs and the analytes used in this work. The arrow indicates the excitation wavelength. (e) Raman background of the PDMS that constitutes the microfluidic channels and characteristic SERS spectra of the analytes: astra blue (AB), toluidine blue (TB), crystal violet (CV), and Nile blue (NB).

samples (which were previously bubbled into a solution), among others.<sup>26,27</sup> Unfortunately, most of these experiments have been carried out for single analytes, which limits their applicability. In this Letter, we present a SERS microfluidic setup designed and tested for the online dual-channel multiplex identification of molecules, using silver nanoparticles as Raman enhancers inside of the microfluidic channel.

Online SERS detection was carried out in different microfluidic devices including T or + shapes (Figure 1a,b). Microfluidic devices were fabricated using conventional soft lithography methods, comprising PDMS on PDMS substrates,<sup>28</sup> giving rise to reproducible, robust, but versatile devices that are transparent to light. The strong electromagnetic fields required for SERS were generated by citrate-capped colloidal silver nanoparticles, which were selected because they can be fabricated in large quantities with outstanding optical performance.<sup>29</sup> These colloids comprise quasi-spherical particles with sizes ranging between 20 and 40 nm, with a LSPR maximum at 409 nm (Figure 1c,d).

We devised a first online experiment to confirm the feasibility of our SERS microfluidic setup to effectively identify analytes within the flow channel. Figure 1a depicts the dimensions and shape of the simplest chip that was used for this first online experiment. The T-shaped microchip features one inlet for the introduction of the silver nanoparticle colloid and another for the introduction of the sample, in this case, an aqueous solution of astra blue (AB, Figure 1d,e).<sup>30</sup> Both channels were operated at the same flow rates of  $100 \mu\text{L h}^{-1}$ . A close look at the optical and SERS mapping images of the T-shaped chip (Figure 2a) shows that the vibrational signatures of the analyte (AB) can be recorded in real time, with SERS acquisition exposure times as low as 70 ms. However, it should be noted that the SERS signal is concentrated at the left-hand side of the flow, with a signal decay toward the right-hand side. On the contrary, no SERS signals from AB were detected at the right-hand side region. This observation is consistent with the presence of a laminar flow inside of the microchannel.

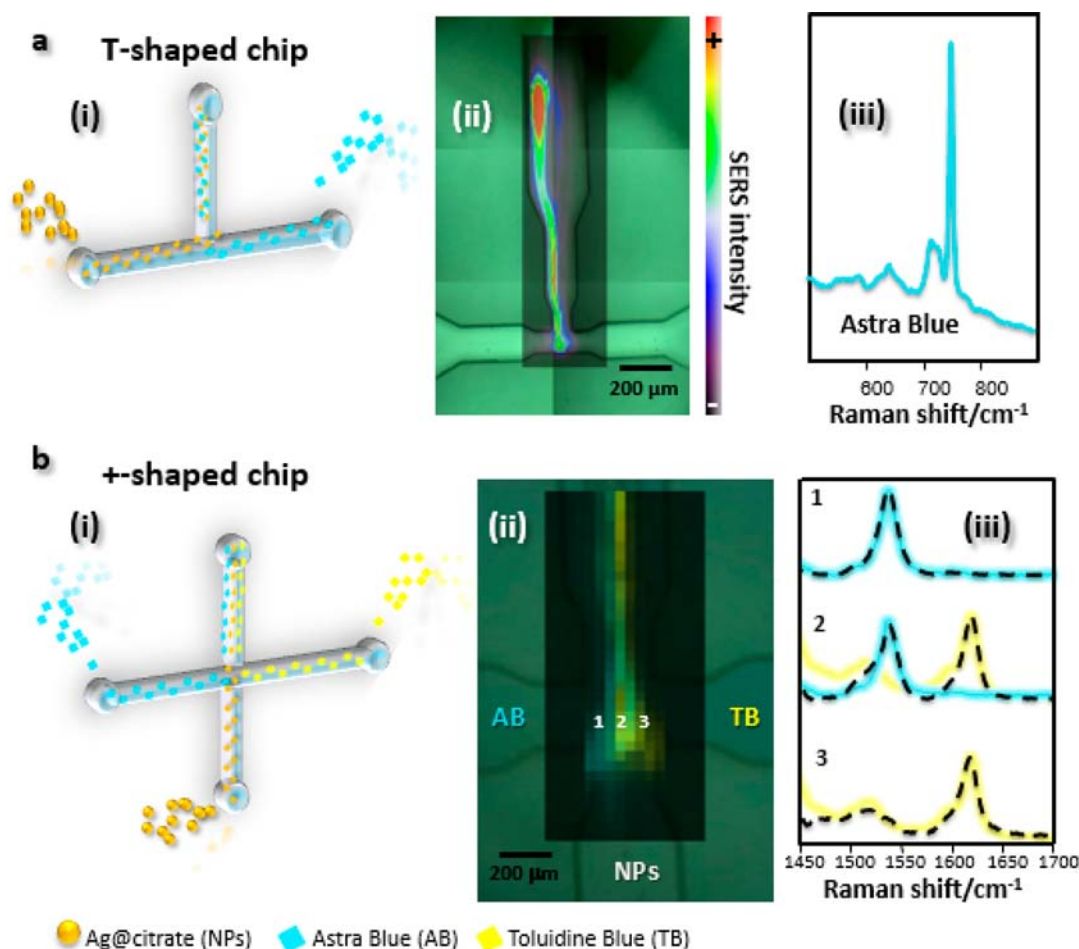


**Figure 2.** (a) T-shaped microfluidic device. (i) Scheme of the microfluidic device depicting the mixing of AB and Ag nanoparticles; (ii) superimposed optical image and SERS mapping of the chip showing the SERS signal intensity of the analyte along the different regions of the channel; and (iii) the characteristic spectra of AB. (b) A +-shaped microfluidic device for dual online monitoring of two flows from different sources (i) containing either AB or toluidine blue (TB); (ii) an optical image and SERS mapping of the microchannel showing the distribution of the analytes (AB, blue; TB, yellow); (iii) SERS spectra obtained from the points labeled with numbers in the image (experimental: dotted black line; references: colored solid lines). Dye concentration, 1 mM; scan time, 70 ms.

The flow of a fluid through a microfluidic channel can be characterized by the Reynolds number,  $Re = Lv\rho/\mu$ , where  $v$  is the average velocity,  $\mu$  is the viscosity,  $\rho$  is the density of the fluid, and  $L$  is the characteristic linear dimension of the channel, in our case, equivalent to  $4A/P$ , where  $A$  and  $P$  are the cross-sectional and the wetted perimeters of the channel, respectively. In the case of this particular experiment using the T-shaped chip, the value of  $Re$  is 0.25, which is indicative of an almost perfect laminar flow, as expected in microfluidics. Under such conditions, the mixture of the nanoparticles with the analyte, which is required to form a SERS-active analyte–nanoparticle complex, is dominated by diffusion. As the dye molecules are smaller than the silver nanoparticles flowing on the right-hand side of the channel, the former are more likely to diffuse toward the left-hand side faster than the nanoparticles do toward the right-hand side. This is in agreement with the SERS mapping profile shown in Figure 2a, in which the area displaying the SERS signal corresponding to AB is located at the left-hand side (Ag colloid laminar flow) and it broadens as the flow penetrates inside of the channel. Additionally, as previously reported, the presence of the analyte induces aggregation in the particle flow with the consequential formation of hot spots and, thus, the increase in SERS intensity.<sup>24,25</sup>

Taking into consideration the previous observations, we designed a new chip containing an additional inlet, that is, a +-shaped microfluidic device comprising two inlets for the flow of two different samples, one inlet for the nanoparticle colloid, and the outlet (Figure 2b). The flow rate was raised to  $500 \mu\text{L h}^{-1}$ , giving rise to a  $Re$  number of 0.61, which again characterizes the flow as highly laminar. This second chip thus features the introduction two analytes, AB and toluidine blue (TB, Figure 1d,e),<sup>30,31</sup> one from each sample flow. Figure 2b shows the optical image and SERS mapping that depicts the distribution of the analytes through the flow. Notably, the spectra acquired from the left-hand side region of the flow only show vibrational signatures corresponding to AB, whereas in the right-hand side region, only TB can be found. Interestingly, the spectra recorded from the central region display the vibrational bands corresponding to both analytes. Again, the SERS intensities of the analytes at both sides of the flow decrease from the center to the side wall and increase as the flow continues, indicating a diffusion-limited mechanism. The diffusion of the dye molecules can be observed, from the lateral sides toward the central flow carrying the silver nanoparticles that enhance the Raman signal. This experiment illustrates the possibility of using a single microfluidic device to monitor

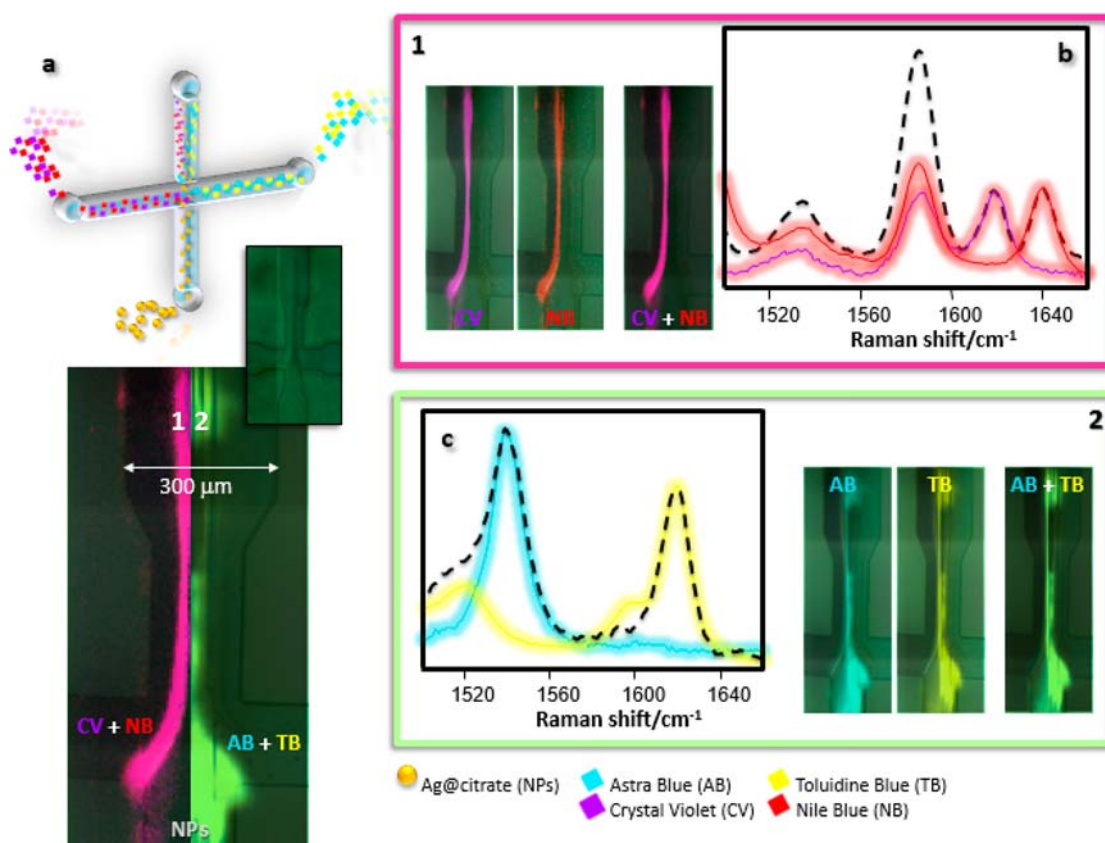


**Figure 3.** (a) A +-shaped microfluidic device for dual multiplex online monitoring of two flows of different sources. Each flow contains a mixture of two different analytes, either CV and NB or AB and TB. (b,c) Optical and SERS images of the microchannel showing the distribution of the analytes (CV + NB, pink; AB + TB, light green; CV, purple; NB, red; AB, blue; and TB, yellow). SERS spectra obtained from the points highlighted in the image (experimental: dotted black line; spectral references: colored solid lines). Dye concentration, 1 mM; scan time, 70 ms.

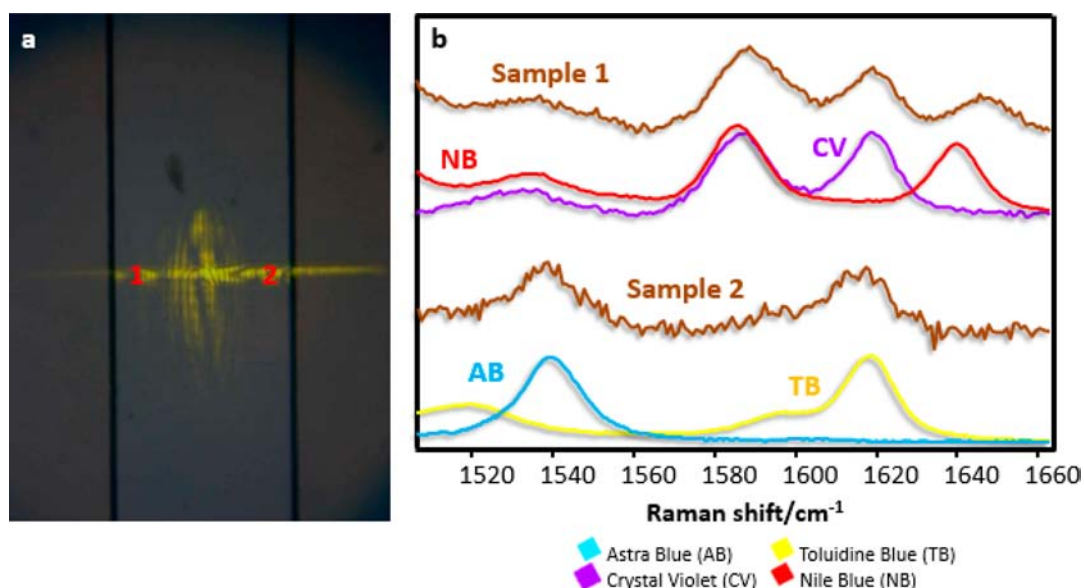


**Figure 4.** A +-shaped microfluidic device for dual multiplex online monitoring of two flows of different sources. Each flow contains a mixture of two different analytes, either CV and NB or AB and TB. (a) Optical image showing the laser. (b) Representative SERS obtained from the points marked in the image. Dye concentration, 0.9 nM; scan time, 10 s.

several sample flows simultaneously, obtaining real time data that can be ascribed to the correct flow source.

To take advantage of the laminar flows generated in the microfluidic devices and the characteristic vibrational signatures

provided by SERS, a new experiment was devised to demonstrate the application of the device for simultaneously monitoring different flows, each containing more than one analyte. To do this, we exploited the +-shaped chip with lower

flow rates in order to decrease the diffusion velocity of samples introduced in both branches. Selected flow rates for this experiment were 100 and 200  $\mu\text{L h}^{-1}$  for the dyes and silver nanoparticles, respectively. Under the given flow rates, the  $Re$  is 0.18, indicating again the high laminar regime that occurred in the microfluidic device. For this experiment, four dyes were selected, crystal violet (CV),<sup>32</sup> Nile blue (NB),<sup>33</sup> AB,<sup>30</sup> and TB (Figure 1d,f).<sup>31</sup> Notably, all of these dyes present electronic absorptions in the visible but far away from the selected excitation laser line (785 nm), thereby avoiding resonant effects in the SERS measurements. Solutions of CV and NB and AB and TB were introduced through the left and right inlets, respectively. To illustrate the distribution of the analytes in the flows, a fast SERS mapping of concentrated solutions (mM) was carried out along the area of the outlet channel of the microchip. Interestingly, both the optical and SERS images for all of the analytes show two well-differentiated regions (see Figure 3), the left-hand side containing only vibrational signals of CV and NB while the right-hand area exclusively contains the signals corresponding to AB and TB. The SERS images of the individual analytes show that each of them is restricted to the region from where it was introduced, without contamination of other areas. Further, the SERS spectra clearly demonstrate that it is possible to recognize the presence of each analyte within a given flow.

This experiment shows the potential of microfluidics for the multiplex monitoring of several flows simultaneously. Because the concentrations of the target analytes (mM) cannot be considered diluted in the experiments so far, we devised an additional detection scheme to study the detection limits and therefore the potential impact of our device as an online multiplex ultradetection tool. A laser beam was focused through a 10 $\times$  objective perpendicularly to the outlet microchannel (Figure 4a). By using a 2D-CCD camera as the detector, the spatial resolution of the spectroscopic signal is defined by the objective used for laser focusing, 10  $\mu\text{m}$  in this case. Then, two solutions, one containing CV and NB and the other TB and CV, were injected through each sample channel. The concentrations of the solutions were varied from mM to pM, and the time for each collection was set to 10 s. Figure 4b shows that the target analytes are fully recognizable in the flowing solution at concentrations down to the nM range (Figure 4b), thereby demonstrating the potential of coupling SERS with microfluidics for ultrasensitive online multiplex monitoring, in full agreement with recent literature.<sup>34</sup>

In summary, we have taken advantage of the combination of the high intensity and complex signals provided by SERS with the flow characteristics of specific microfluidic channels to engineer a microdevice that is capable of multiplex monitoring of samples from different sources in real time. This new family of devices may pave the road for remote real time monitoring of environmental samples such as natural or waste waters and to the high-throughput screening of multiple samples in healthcare analysis.

## EXPERIMENTAL MATERIALS AND METHODS

**Materials.** Unless otherwise stated, all chemicals were purchased from Sigma-Aldrich. Glassware was cleaned with aqua regia and extensively washed with water. Milli-Q water (Millipore) was used throughout all of the experiments.

**AgNPs Synthesis.** The synthesis of the silver nanoparticles was carried out according to the generalized Lee–Meisel reduction method.<sup>35</sup> Briefly, 2 mL of 1% sodium citrate solution was

added to a 100 mL  $\text{AgNO}_3$   $10^{-3}$  M boiling solution. The mixture was kept boiling for 1 h until a gray–green turbid color appeared.

**Device Fabrication.** The microfluidic PDMS/glass device was fabricated by conventional soft lithography methods.<sup>28</sup> Briefly, the device was first devised with Autocad 2007 (Autodesk), and a dark-field mask was printed (Circuitgraphics). SU-8 2025 photoresist (Micro-Chem) was spin-coated onto a silicon wafer (diameter: 76.2 mm, Compant Technology Ltd.) at 500 rpm for 5 s and then ramped to 1000 rpm at an acceleration of 300 rpm  $\text{s}^{-1}$  for 33 s. The final thickness of the photoresist was measured by profilometry on the finished master (DekTak 150). The wafer was subsequently prebaked for 3 min at 65  $^\circ\text{C}$ , then 9 min at 95  $^\circ\text{C}$ , and finally 3 min at 65  $^\circ\text{C}$ . Then, it was exposed to UV light through the mask on a mask aligner (MJB4, Suss Microtech). After postbaking and development, the master was hard-baked for 1 min at 170  $^\circ\text{C}$ . A mixture of poly(dimethylsiloxane) (PDMS, Sylgard 184) and cross-linker (ratio 10: 1, w/w) was poured over the master, degassed for 30 min, and then cured overnight at 75  $^\circ\text{C}$ . The cured device was cut and peeled from the master, and holes for tubing were made with a biopsy punch. After treatment with air plasma for 30 s, the device was bound to another piece of PDMS produced by the same procedure but without holes in order to close the microfluidic system. The device was baked at 90  $^\circ\text{C}$  for 30 min to make permanent the sealing. Finally, the microfluidic channels were treated with Aquapel (Pittsburgh, U.S.), a commercially available fluorosilane, followed by flushing of the channels with fluorosilane.

**Microfluidic Experiments.** Flows in all of the chips were driven with Harvard Apparatus 2000 syringe infusion pumps. Plastic syringes of 1 mL (Braun) were used in all cases, both for the dyes and for the silver nanoparticles. The syringes were connected via polyethylene tubing (Intramedic, i.d. 0.38 mm) to the device. The concentration of the individual dye solutions in water (experiments 1 and 2) was of  $10^{-3}$  M, and the concentration of the mixed dye solutions used in experiment 3 was of  $5 \times 10^{-3}$  M. These solutions were subsequently diluted to pM concentration to perform the ultradetection experiments. The AgNPs were dispersed in water in a concentration of  $10^{-3}$  M. Different flow rates were used in the three respective online experiments. In the case of the first experiment, the flow rate was 100  $\mu\text{L h}^{-1}$  for both the AgNPs and the dye AB. When dealing with the +-shaped chip in the second experiment, the flow rates were 500  $\mu\text{L h}^{-1}$  for the dyes and the AgNPs. Finally, in both multiplex detection experiments, the flow rate for the side channels flowing the dye mixtures was 100  $\mu\text{L h}^{-1}$ , and that for the AgNPs was 200  $\mu\text{L h}^{-1}$ . The experiment was carried out at room temperature, neglecting the laser heating during the measurement.

**Characterization.** Optical characterization was carried out by UV/vis/NIR spectroscopy with a Cary 5000 spectrophotometer. TEM images were obtained with a JEOL JEM 1010 transmission electron microscope operating at an acceleration voltage of 100 kV. Optical images of the microfluidic devices were obtained with a Nikon microscope through a 5 $\times$  objective.

**Surface-Enhanced Raman Scattering Spectroscopy.** SERS experiments were conducted in a micro-Renishaw InVia Reflex system. The spectrograph uses a high-resolution grating (1200 grooves  $\text{mm}^{-1}$ ) with additional band-pass filter optics, a confocal microscope, and a 2D-CCD camera. A laser excitation energy of 785 nm (diode) was used for all of the online

measurements. The online mappings presented in this work were carried out in a confocal microscope in backscattering geometry using 5X objectives. SERS maps were collected in the outlet channel region by means of the Renishaw StreamLine accessory with step sizes of 25  $\mu\text{m}$  and detection times of 70 ms. Ultrasensitive detection was carried out with the linear laser focused perpendicularly to the outlet channel through a 10X objective. The step size was 10  $\mu\text{m}$ , and the detection times were 10 s.

## AUTHOR INFORMATION

### Corresponding Authors

\*E-mail: llizmarzan@cicbiomagune.es (L.M.L.-M.).

\*E-mail: ramon.alvarez@urv.cat (R.A.A.-P.).

### Notes

The authors declare no competing financial interest.

## ACKNOWLEDGMENTS

This work was funded by the Spanish Ministerio de Economía y Competitividad (CTQ2011-23167, MAT2010-15374) and the European Research Council (ERC Advanced Grant PLASMAQUO, FP7MC-IEF 329131).

## REFERENCES

- (1) Theberge, A. B.; Courtois, F.; Schaerli, Y.; Fischlechner, M.; Abell, C.; Hollfelder, F.; Huck, W. T. S. Microdroplets in Microfluidics: An Evolving Platform for Discoveries in Chemistry and Biology. *Angew. Chem., Int. Ed.* **2010**, *49*, 5846–5868.
- (2) Casadevall i Solvas, X.; deMello, A. Droplet Microfluidics: Recent Developments and Future Applications. *Chem. Commun.* **2011**, *47*, 1936–1942.
- (3) Craighead, H. Future Lab-on-a-chip Technologies for Interrogating Individual Molecules. *Nature* **2006**, *442*, 387–393.
- (4) Whitesides, G. M. The Origins and the Future of Microfluidics. *Nature* **2006**, *442*, 368–373.
- (5) Houbart, V.; Cobraiville, G.; Lecomte, F.; Debrus, B.; Hubert, P.; Fillet, M. Development of a Nano-Liquid Chromatography on Chip Tandem Mass Spectrometry Method for High-Sensitivity Hepcidin Quantitation. *J. Chromatogr., A* **2011**, *1218*, 9046–9054.
- (6) Sikanen, T.; Franssila, S.; Kauppila, T. J.; Kostianen, R.; Kotiaho, T.; Ketola, R. A. Microchip Technology in Mass Spectrometry. *Mass Spectrosc. Rev.* **2010**, *29*, 351–391.
- (7) Mogensen, K. B.; Kutter, J. P. Optical Detection in Microfluidic Systems. *Electrophoresis* **2009**, *30*, S92–S100.
- (8) Horrocks, M. H.; Li, H.; Shim, J.-U.; Ranasinghe, R. T.; Clarke, R. W.; Huck, W. T. S.; Abell, C.; Klenerman, D. Single Molecule Fluorescence under Conditions of Fast Flow. *Anal. Chem.* **2011**, *84*, 179–185.
- (9) De Leebeek, A.; Kumar, L. K. S.; de Lange, V.; Sinton, D.; Gordon, R.; Brolo, A. G. On-Chip Surface-Based Detection with Nanohole Arrays. *Anal. Chem.* **2007**, *79*, 4094–4100.
- (10) Yakovleva, J.; Davidsson, R.; Bengtsson, M.; Laurell, T.; Emnéus, J. Microfluidic Enzyme Immunosensors with Immobilised Protein A and G Using Chemiluminescence Detection. *Biosens. Bioelectron.* **2003**, *19*, 21–34.
- (11) Kimura, S.; Fukuda, J.; Tajima, A.; Suzuki, H. On-Chip Diagnosis of Subclinical Mastitis in Cows by Electrochemical Measurement of Neutrophil Activity in Milk. *Lab Chip* **2012**, *12*, 1309–1315.
- (12) Stedtfeld, R. D.; Tourlousse, D. M.; Seyrig, G.; Stedtfeld, T. M.; Kronlein, M.; Price, S.; Ahmad, F.; Gulari, E.; Tiedje, J. M.; Hashsham, S. A. Genex: A Device for Point of Care Genetic Testing Using a Smartphone. *Lab Chip* **2012**, *12*, 1454–1462.
- (13) deMello, A. J. Control and Detection of Chemical Reactions in Microfluidic Systems. *Nature* **2006**, *442*, 394–402.
- (14) Segerink, L. A Low-Cost 2D Fluorescence Detection System for Micro-Sized Beads On-Chip. *Lab Chip* **2012**, *12*, 1780–1783.
- (15) Dittrich, P. S.; Manz, A. Single-Molecule Fluorescence Detection in Microfluidic Channels—The Holy Grail in  $\mu\text{tas}$ ? *Anal. Bioanal. Chem.* **2005**, *382*, 1771–1782.
- (16) Dittrich, P. S.; Tachikawa, K.; Manz, A. Micro Total Analysis Systems. Latest Advancements and Trends. *Anal. Chem.* **2006**, *78*, 3887–3908.
- (17) Götz, S.; Karst, U. Recent Developments in Optical Detection Methods for Microchip Separations. *Anal. Bioanal. Chem.* **2007**, *387*, 183–192.
- (18) Rodriguez-Lorenzo, L.; Fabris, L.; Alvarez-Puebla, R. A. Multiplex Optical Sensing with Surface-Enhanced Raman Scattering: A Critical Review. *Anal. Chim. Acta* **2012**, *745*, 10–23.
- (19) Lim, C.; Hong, J.; Chung, B. G.; deMello, A. J.; Choo, J. Optofluidic Platforms Based on Surface-Enhanced Raman Scattering. *Analyst* **2010**, *135*, 837–844.
- (20) Tong, L.; Righini, M.; Gonzalez, M. U.; Quidant, R.; Kall, M. Optical Aggregation of Metal Nanoparticles in a Microfluidic Channel for Surface-Enhanced Raman Scattering Analysis. *Lab Chip* **2009**, *9*, 193–195.
- (21) Gao, R.; Choi, N.; Chang, S. I.; Kangle, S. H.; Song, J. M.; Cho, S. I.; Lim, D. W.; Choo, J. Highly Sensitive Trace Analysis of Paraquat Using a Surface-Enhanced Raman Scattering Microdroplet Sensor. *Anal. Chim. Acta* **2010**, *681*, 87–91.
- (22) Choo, J.; Lim, C.; Chen, L.; Chon, H.; Wang, G.; Hong, J.; deMello, A. J. Surface-Enhanced Raman Scattering in Nanoliter Droplets: Towards High-Sensitivity Detection of Mercury (II) Ions. *Anal. Bioanal. Chem.* **2009**, *394*, 1827–1832.
- (23) Lee, S. J.; Moskovits, M. Visualizing Chromatographic Separation of Metal Ions on a Surface-Enhanced Raman Active Medium. *Nano Lett.* **2011**, *11*, 145–150.
- (24) Piorek, B. D.; Lee, S. J.; Moskovits, M.; Meinhart, C. D. Free-Surface Microfluidics/Surface-Enhanced Raman Spectroscopy for Real-Time Trace Vapor Detection of Explosives. *Anal. Chem.* **2012**, *84*, 9700–9705.
- (25) Piorek, B. D.; Seung, J. L.; Santiago, J. G.; Moskovits, M.; Banerjee, S.; Meinhart, C. D. Free-Surface Microfluidic Control of Surface-Enhanced Raman Spectroscopy for the Optimized Detection of Airborne Molecules. *Proc. Natl. Acad. Sci. U.S.A.* **2007**, *104*, 18898–18901.
- (26) Oh, Y.-J.; Park, S.-G.; Kang, M.-H.; Choi, J.-H.; Nam, Y.; Jeong, K.-H. Beyond the SERS: Raman Enhancement of Small Molecules Using Nanofluidic Channels with Localized Surface Plasmon Resonance. *Small* **2011**, *7*, 184–188.
- (27) Ackermann, K. R.; Henkel, T.; Popp, J. Quantitative Online Detection of Low-Concentrated Drugs via a SERS Microfluidic System. *ChemPhysChem* **2007**, *8*, 2665–2670.
- (28) Xia, Y.; Whitesides, G. M. Soft Lithography. *Angew. Chem., Int. Ed.* **1998**, *37*, 550–575.
- (29) Alvarez-Puebla, R. A.; Aroca, R. F. Synthesis of Silver Nanoparticles with Controllable Surface Charge and Their Application to Surface-Enhanced Raman Scattering. *Anal. Chem.* **2009**, *81*, 2280–2285.
- (30) Wustholz, K. L.; Brosseau, C. L.; Casadio, F.; Van Duyne, R. P. Surface-Enhanced Raman Spectroscopy of Dyes: From Single Molecules to the Artists' Canvas. *Phys. Chem. Chem. Phys.* **2009**, *11*, 7350–7359.
- (31) Rodríguez-Lorenzo, L.; Krpetic, Z.; Barbosa, S.; Alvarez-Puebla, R. A.; Liz-Marzán, L. M.; Prior, I. A.; Brust, M. Intracellular Mapping with SERS-Encoded Gold Nanostars. *Integr. Biol.* **2011**, *3*, 922–926.
- (32) Aldeanueva-Potel, P.; Correa-Duarte, M. A.; Alvarez-Puebla, R. A.; Liz-Marzán, L. M. Free-Standing Carbon Nanotube Films as Optical Accumulators for Multiplex SERRS Attomolar Detection. *ACS Appl. Mater. Interface* **2010**, *2*, 19–22.
- (33) Fernández-López, C.; Mateo-Mateo, C.; Alvarez-Puebla, R. A.; Pérez-Juste, J.; Pastoriza-Santos, I.; Liz-Marzán, L. M. Highly Controlled Silica Coating of PEG-Capped Metal Nanoparticles and

Preparation of SERS-Encoded Particles. *Langmuir* **2009**, *25*, 13894–13899.

(34) Negri, P.; Jacobs, K. T.; Dada, O. O.; Schultz, Z. D. Ultrasensitive SERS Flow Detector Using Hydrodynamic Focusing. *Anal. Chem.* **2013**, *85*, 10159–10166.

(35) Lee, P. C.; Meisel, D. Adsorption and Surface-Enhanced Raman of Dyes on Silver and Gold Sols. *J. Phys. Chem.* **1982**, *86*, 3391.